HHS Public Access

Author manuscript

J Physiol. Author manuscript; available in PMC 2022 April 12.

Published in final edited form as:

J Physiol. 2020 April ; 598(8): 1625–1639. doi:10.1113/JP278933.

Reduced Na^+K^+-ATPase activity may reduce amino acid uptake in IUGR fetal sheep muscle despite unchanged *ex vivo* amino acid transporter activity

Jane Stremming[1], **Thomas Jansson**[2], **Theresa L Powell**[1,2], **Paul J Rozance**[1], **Laura D Brown**[1]

[1]Department of Pediatrics, University of Colorado Anschutz Medical Campus, Aurora, CO

[2]Department of Obstetrics and Gynecology, University of Colorado Anschutz Medical Campus, Aurora, CO

Abstract

Fetuses with intrauterine growth restriction (IUGR) have lower muscle mass that persists postnatally. Using a sheep model of placental insufficiency and IUGR, we have previously demonstrated lower net total uptake of amino acids by the fetal hindlimb and lower skeletal muscle protein synthesis rates. To investigate the mechanisms underlying these changes, we tested the hypothesis that *ex vivo* amino acid transporter and Na^+K^+-ATPase activity is reduced, and *ex vivo* ATP levels are lower in hindlimb skeletal muscle of the IUGR fetus. We developed a novel protocol to measure transporter mediated histidine uptake, system L amino acid transporter activity, and Na^+K^+-ATPase activity using sarcolemmal membranes isolated from hindlimb muscle of control (CON, n=11–12) and IUGR (n=12) late gestation fetal sheep. We also determined ATP content and the activity of insulin and mTOR signaling, which are involved in regulating cellular amino acid uptake and protein synthesis, by measuring the expression and phosphorylation of AKT, 4E-BP1, eIF2α, AMPKα, p70 S6 kinase and rpS6 in muscle homogenates. Transporter mediated histidine uptake and system L activity were similar in control and IUGR sarcolemma, but *ex vivo* Na^+K^+-ATPase activity was lower by 64% (P=0.019) in IUGR sarcolemma. ATP content was lower by 25% (P=0.007) in IUGR muscle. Insulin, AMPK, and mTOR signaling activity was similar in control and IUGR muscle. We speculate that reduced muscle sarcolemmal Na^+K^+-ATPase activity and lower ATP content diminishes the sodium gradient *in vivo*, resulting in a reduced driving force for sodium dependent transporters and subsequently lower muscle amino acid uptake.

Corresponding Author: Laura Brown, Perinatal Research Center, 13243 East 23rd Avenue, Aurora, CO, 80045; laura.brown@cuanschutz.edu.

Author Contributions:

Conception or design of the work: JS, TJ, TLP, PJR, LDB

Acquisition of data: JS

Data analysis/interpretation of data: JS, TJ, TLP, PJR, LDB

Drafting and revising the work critically for important intellectual content: JS, TJ, TLP, PJR, LDB

All authors have approved to the final version of the manuscript and agree to be accountable for all aspects of the work. All authors listed qualify for authorship, and all authors who qualify are listed.

Additional Information

Competing Interests: All authors have no conflicts of interest to disclose.

Keywords

Fetal development; fetal programming; skeletal muscle; Placenta; Pregnancy; Perinatal Physiology

INTRODUCTION

Intrauterine growth restriction (IUGR) is defined as the failure to reach the full genetically determined fetal growth potential and is associated with increased perinatal morbidity and mortality (Sharma et al., 2016) and risk of developing metabolic disease, such as diabetes and obesity, in adulthood (Srikanthan & Karlamangla, 2011; Thorn et al., 2011). Fetuses with IUGR are born with reduced muscle mass that can persist postnatally (Gale et al., 2001; Kensara et al., 2005; Brown & Hay, 2016). Reductions in skeletal muscle growth in utero have important implications for lifelong metabolic health because lower birth weight and lean mass can lead to reduced peripheral glucose disposal and insulin sensitivity, both contributors to type 2 diabetes (Whincup et al., 2008; Srikanthan & Karlamangla, 2011; Thorn et al., 2011; Brown & Hay, 2016).

In a well-established sheep model of placental insufficiency and IUGR that allows for chronic catheterization of the fetal hindlimb, we previously demonstrated that total net amino acid uptake rates and linear growth rate of the IUGR hindlimb were lower than in normally-grown control (CON) fetuses (Rozance et al., 2018). Hindlimb oxygen delivery and consumption rates were lower in IUGR compared to control fetuses, yet weight-specific blood flow was similar between groups, consistent with the hypothesis that hindlimb growth slows to match blood flow and oxygen availability. Skeletal muscle protein accretion rates and fractional protein synthetic rates also were reduced in the IUGR hindlimb, but protein breakdown rates were unchanged (Rozance et al., 2018). Placental amino acid transporter capacity, including the activity of the system A and system L families of transporters, has been reported to be decreased in placentas of IUGR humans and in a wide range of animal models of IUGR (Jansson & Powell, 2006; Kavitha et al., 2014; Pantham et al., 2015). In IUGR induced by maternal heat exposure in sheep, placental capacity to transport essential amino acids such as leucine (Ross et al., 1996) and threonine (Anderson et al., 1997), and a branched-chain amino acid analog, aminocyclopentane-1-carboxylic acid (ACP) (de Vrijer et al., 2004), is reduced. However, despite impaired placental amino acid transport, there are minimal differences in plasma amino acid concentrations between control and IUGR fetal sheep at 90% gestation (Regnault et al., 2013; Rozance et al., 2018). Therefore, reduced amino acid uptake and protein accretion rates by the IUGR fetal hindlimb are not the direct result of lower plasma amino acid concentrations, but may be due to lower activity of amino acid uptake transporters in the sarcolemma and/or lower skeletal muscle utilization of amino acids by IUGR animals (Regnault et al., 2013; Rozance et al., 2018).

Which specific amino acid uptake transporters are expressed and active in fetal skeletal muscle is largely unknown. System A, N, and L amino acid transporters are present in the postnatal skeletal muscle sarcolemma and facilitate net uptake of neutral amino acids into the myocyte (Hundal et al., 1987; Mackenzie & Erickson, 2004; Verrey et al., 2004). System A and N constitute the *SLC38* gene family of sodium coupled neutral amino

acid transporters. These transporters are dependent on a sodium gradient, established by Na^+K^+-ATPase, for co-transport of sodium and amino acids into the cell and are highly sensitive to changes in pH within the physiological range with inhibition of transporter activity at lower pH (Broer, 2014). System A amino acid transporters, such as SNAT2 (*SLC38A2*) and SNAT4 (*SLC38A4*), transport small neutral amino acids including alanine, serine, glutamine, asparagine, histidine, and cysteine (Broer, 2014). System N amino acid transporters, such as SNAT3 (*SLC38A3*), SNAT5 (*SLC38A5*), and SNAT7 (*SLC38A7)* have a preference for glutamine, serine, asparagine, and histidine (Broer, 2014). System L amino acid transporters, such as LAT1 (*SLC7A5*) and LAT2 (*SLC7A8*), are sodium independent transporters that exchange small neutral amino acids for branched chain amino acids including leucine, isoleucine, and valine, and large neutral amino acids such as phenylalanine and tryptophan (Barker & Ellory, 1990; Verrey, 2003). CD98 (*SLC3A2*), also known as heavy subunit 4F2hc, is a glycoprotein that binds with system L transporters (Verrey, 2003).

Importantly, because the net cellular uptake of essential amino acids by system L requires the exchange with intracellular amino acids, the activity of system L is dependent on the availability of amino acids in the cytosol (Verrey, 2003), which is governed by sodium dependent transporters such as system A and system N (Broer, 2014) (Figure 1). Thus, changes in the activity of transporters mediating active transport of non-essential amino acids into the cell may indirectly modify system L activity. The impact of IUGR on fetal skeletal muscle amino acid transporter expression and activity is unknown.

We hypothesized that *ex vivo* amino acid transporter and Na^+K^+-ATPase activity is reduced, and *ex vivo* ATP levels are lower in hindlimb skeletal muscle of the IUGR fetus. Our approach was to develop a novel protocol to measure amino acid transporter mediated histidine uptake, system L amino acid transporter activity, and Na^+K^+-ATPase activity using sarcolemma isolated from the hindlimb muscle of control and IUGR late gestation fetal sheep. We also measured ATP content and determined the activity of insulin and mTOR signaling, which are involved in regulating cellular amino acid uptake and protein synthesis, by measuring the expression and phosphorylation of AKT, 4E-BP1, eIF2α, AMPKα, p70 S6 kinase, and rpS6 in whole muscle homogenate.

METHODS

Ethical approval

Study protocols were approved by the Institutional Animal Care and Use Committee at the University of Colorado Anschutz Medical Campus (Protocol #77614101E) and are in compliance with guidelines from the American Association for the Accreditation of Laboratory Animal Care (AAALAC) International. All experiments conform to the principles and regulations as described by Grundy (Grundy, 2015). The investigators understand the ethical principles under which the journal operates and confirm that their work complies with this animal ethics checklist. Experiments were performed at the Perinatal Research Facility (PRF) on the Anschutz Medical Campus.

Animal care

Pregnant Columbia-Rambouillet mixed-breed sheep (Nebeker Ranch, Lancaster, CA) were housed in environmental chambers and exposed to elevated ambient temperatures (40°C for 12 h; 35°C for 12 h) and 40% humidity from 38 days gestation (dga, term = 147 dga) to 116 dga to induce placental insufficiency and intrauterine growth restriction (IUGR group; n=13) (Bell et al., 1987; Brown et al., 2012). Control ewes were housed in similar environmental chambers at the PRF but were exposed to normal ambient temperatures and humidity (CON group; n=12). After environmental treatment, all sheep were exposed to normal ambient temperatures and humidity for the remainder of the studies. All sheep were given *ad libitum* access to water. Maternal food intake was similar between control and IUGR groups (Rozance et al., 2018; Wai et al., 2018). All sheep were pregnant with singleton fetuses, with the exception of one triplet in the IUGR group that was incidentally found at the time of necropsy (Rozance et al., 2018). This triplet was included in the IUGR data set, because it was not an outlier for fetal weight or any other physiological parameter within the IUGR group.

Surgical procedure

Late gestation pregnant sheep underwent maternal laparotomy and hysterotomy under general anesthesia for fetal and maternal catheter placement as previously reported in detail (Rozance et al., 2018; Wai et al., 2018). Ewes were given diazepam (0.2 mg/kg) and ketamine (20 mg/kg) through a superficial vein to induce general anesthesia, and they were maintained on isoflurane inhalation anesthesia (2–4%) for the duration of the surgical procedure. Depth of anesthesia was determined and maintained in response to corneal reflex, toe pinch, assessment of jaw tone in the mother and muscle tone in the fetus, and continuous pulse oximetry and heart rate monitoring. Ewes were given Penicillin G procaine (600,000 units intramuscularly) prior to surgery. In 8 ewes with control fetuses and 13 ewes with IUGR fetuses, polyvinyl catheters were placed in the fetal lamb with the tips positioned in the external iliac artery, distal inferior vena cava, and in the femoral vein (Rozance et al., 2018). Because of the variability associated with transporter activity assays, we collected gastrocnemius muscle from four additional control fetuses (Wai et al., 2018). In those animals, environmental chamber treatment was performed as described above, and polyvinyl catheters were placed in the fetus with the tips positioned in the external iliac artery, distal inferior vena cava, and the umbilical vein (Wai et al., 2018). Ampicillin (500 mg) was injected into the amniotic fluid prior to surgical closure. In all animals, catheters were tunneled subcutaneously to the maternal flank. Ewes received banamine (2.2 mg/kg divided twice per day intramuscularly) on the day of surgery and the two following days. Animals were allowed to recover following surgery for a minimum of 5 days prior to metabolic study. Physiological measurements, including fetal plasma substrates and steady-state substrate uptake rates by the fetal hindlimb or whole fetus as well as metabolic hormone concentrations, were reported previously (Rozance et al., 2018; Wai et al., 2018). External iliac arterial and femoral venous potassium concentrations were measured using an ABL blood gas analyzer (Radiometer, Brea, CA) and are reported herein.

Skeletal muscle collection

After conclusion of the metabolic study on day 134–137 of gestation, ewes received diazepam (0.2 mg/kg) and ketamine (20 mg/kg) intravenously, and fetuses were delivered via maternal laparotomy and hysterotomy. The biceps femoris muscle was exposed, and a biopsy was obtained from the anesthetized fetus and immediately frozen in liquid nitrogen. Animals were then euthanized by administering intravenous pentobarbital sodium (Fatal Plus; Bortech Pharmaceuticals, Dearborn, MI) to both the mother and the fetus, after which fetal (whole body and individual skeletal muscle) weights were obtained. Fetal muscle biopsies were obtained from the gastrocnemius muscle within 10 minutes of fetal death and snap frozen in liquid nitrogen. Muscle biopsies were hand ground under liquid nitrogen with mortar and pestle and stored at −80°C.

Gene expression

Biopsies of snap frozen biceps femoris muscle were homogenized in Trizol LS (Ambion, Carlsbad, CA). RNA was purified with Qiagen RNeasy Mini Kit (Qiagen, Venlo, Netherlands) and RNase-Free DNAse Set (Qiagen) according to the manufacturer's protocol. RNA was quantified with a spectrophotometer (Nanodrop ND-1000, Thermo Fisher Scientific). Two μg of RNA was converted to cDNA using SuperScript III First-Strand Synthesis System (Invitrogen, Carlsbad CA) according to the manufacturer's protocol. PCR primers were optimized for *SLC38A2, SLC38A3, SLC38A4*, *SLC38A5, SLC38A7, SLC7A5*, *SLC7A8*, and *SLC3A2* (Table #1). Quantitative real time PCR was performed in triplicate using FastStart Universal SYBR Green Master (Roche, Pleasanton, CA) on LightCycler 480 Instrument II (Roche Life Science, Indianapolis, IN) with a relative standard curve of pooled skeletal muscle cDNA. The conditions for amplification were: 95°C for 5 minutes; 95°C for 15 seconds, 60°C for 30 seconds, 72°C for 30 seconds, and melting curve from 60–95°C. Expression levels of *SLC38A2, SLC38A4*, *SLC7A5*, *SLC7A8*, and *SLC3A2* were normalized to the average of beta actin, GAPDH, and S15 expression. Expression levels of *SLC38A3, SLC38A5*, and *SLC38A7* were normalized to the average of beta actin, S15, and RLP37A expression. These experiments and analysis were performed according to the Minimum Information for Publication of Quantitative Real-Time PCR Experiments (MIQE) guidelines (Bustin et al., 2009).

Sarcolemmal membrane vesicle preparation

The protocol for isolating sarcolemma from fetal sheep skeletal muscle was adapted from previous studies (Klip et al., 1987; Ahmed et al., 1990). All steps, including centrifugation, were performed at 4°C or on ice. Up to 2.5 grams of ground gastrocnemius muscle was homogenized for 5 seconds in buffer D [250 mM sucrose in 10 mM hepes-Tris with protease and phosphatase inhibitors (protease inhibitor cocktail, phosphatase inhibitor cocktails 2 and 3, Sigma Aldrich, St. Louis, MO)] with a ratio of 10 mL per gram of tissue. The homogenate was filtered through sterile gauze, and 300 μL of this crude homogenate was saved in aliquots for western blot analysis. The remaining crude homogenate was centrifuged at 1,200 g for 10 minutes. The supernatant was collected and saved on ice. The pellet was resuspended in buffer D (5 mL per gram of starting tissue), hand homogenized, and centrifuged at 1,200 g for 10 minutes. The supernatants were combined and centrifuged at

9,000 g for 10 minutes. The supernatant was then centrifuged at 190,000 g for 120 minutes. The pellet was suspended in 3.1 mL of buffer D and hand homogenized. The suspension was applied to the top of a sucrose gradient (30%, 35%, 40% sucrose) and centrifuged at 100,000 g for 16 hours. The sarcolemma was recovered from the top of the 30% sucrose layer and centrifuged at 190,000 g for 60 minutes. The pellet was resuspended in 150 μL of buffer D. Protein concentration was measured using Pierce BCA Protein Assay Kit (Thermo Fisher Scientific, Waltham, MA).

Sacrolemmal enrichment

Sacrolemmal enrichment was determined by western blot analysis of the expression of the β1 subunit of Na^+K^+-ATPase, a plasma membrane marker. Two μg of protein from the sacrolemmal fraction and 20 μg of protein from the crude homogenate were mixed with beta-mercaptoethanol, heated to 90°C for 5 minutes, and loaded into a precast Tris-HCl 4–15% gel (Biorad Laboratories, Hercules, CA). Electrophoresis was performed and protein was transferred to PVDF membranes (Biorad). Membranes were stained for protein using amido black, which was used to account for any differences in loading and transfer. Membranes were blocked in 5% milk in TBS-T (Tris buffered saline, 0.1% Tween 20) for 1 hour at room temperature. The membrane was incubated with Na^+K^+-ATPase β1 antibody [US Biological Life Sciences, Salem, MA, please see Table #2 for Research Resource Identifiers (RRIDs)] diluted to 1:1000 overnight at 4°C. The membrane was then incubated in HRP-linked anti-mouse secondary antibody (Cell Signaling Technologies, Inc. Danvers, MA) diluted to 1:3000 for 1 hour at room temperature. Bands were visualized using enhanced chemiluminescent substrate (Thermo Scientific) exposed on G:BOX (Syngene, Frederick, MD). The ratio of sarcolemmal/crude homogenate expression of the Na^+K^+-ATPase β1 subunit was used as a measure of enrichment. There was no statistical difference in this ratio between the control (20.97 ± 7.56) and the IUGR group (24.61 ± 4.40) indicating similar sarcolemmal enrichment.

Western blot analysis

Protein expression levels of Na^+K^+-ATPase α1, and total and phosphorylated protein kinase B (AKT, Ser 473), eukaryotic translation initiation factor 4E-binding protein 1 (4E-BP1, Thr 37/46, Thr 70), eukaryotic initiation factor 2 α (eIF2α, Ser 51), AMP-activated protein kinase α (AMPKα, Thr 172), ribosomal protein S6 kinase (p70 S6 kinase, Thr421/Ser424), and ribosomal protein S6 (rpS6, Ser 235/236) were determined by western blot analysis (see Table #2 for RRIDs) and compared between control and IUGR groups. For measurement of Na^+K^+-ATPase α1, 2 μg protein (sarcolemma) was combined with beta-mercaptoethanol, heated to 60°C for 5 minutes, and loaded onto a precast Tris-HCl 4–15% gel (Biorad). For total and phosphorylated AKT, 4E-BP1, eIF2α, and AMPKα, 15 μg protein (crude homogenate from gastrocnemius muscle) was combined with beta-mercaptoethanol, heated to 90°C for 5 minutes, and loaded onto a precast Tris-HCl 4–15% gel (Biorad). Electrophoresis was performed, and protein was transferred to PVDF membranes (Biorad). Membranes were stained for protein using amido black, which was used to account for any differences in loading and transfer. Membranes were blocked in 5% milk in TBS-T for 1 hour at room temperature and subsequently incubated with primary antibody (diluted to 1:1000) in 5% BSA overnight at 4°C. The membranes were incubated in the appropriate

HRP-linked anti-mouse or anti-rabbit secondary antibody (diluted to 1:3000) in BSA for 1 hour at room temperature. Bands were visualized using enhanced chemiluminescent substrate (Thermo Scientific) or Super Signal West Dura (Thermo Scientific) exposed on G:BOX (Syngene). For total and phosphorylated p70 S6 kinase and rpS6, the protocol was similar to the procedure above except: 20 μg protein (crude homogenate) was combined with dithiothreitol, protein was transferred to nitrocellulose membranes (GVS, Sanford, ME), and blocked overnight at 4°C. Bands were visualized using near-infrared fluorescence exposed on Odyssey FC-0788 (LI-COR Biosciences, Lincoln, NE) using goat anti-rabbit secondary antibody (diluted to 1:4000) in 5% milk.

Amino acid transporter activity

Amino acid transporter mediated histidine uptake and system L activity were measured using rapid filtration techniques adapted from previous studies in order to accomplish the measurements with small amounts of sarcolemma (Jansson et al., 2002). Samples were warmed to 37°C in a water bath immediately prior to the experiment. Fifteen μL of vesicles with known protein concentration (range 0.63 to 1 μg/μL) were added to 30 μL of 17 mM Hepes-Tris buffer containing 215 mM NaCl, 2μM ^{3}H-leucine (Perkin Elmer, Waltham, MA), and 100 μM ^{14}C-histidine (Perkin Elmer). Vesicles and buffer were mixed by vortex for 2 seconds. In initial studies, time dependence of uptake of histidine (Figure 2A) and leucine (Figure 2B) was determined to be linear during the first 900 seconds. In all subsequent studies, uptake was stopped after 300 seconds by adding 2 mL of ice cold PBS. The contents were poured over 0.45 μm nitrocellulose filters (Millipore, Burlington, MA) that were presoaked with PBS buffer containing unlabeled L-histidine and L-leucine and rinsed three times with 2 mL of ice cold PBS. Filters were placed in scintillation vials containing 8 mL of filter count scintillation fluid (Perkin Elkins). ^{3}H and ^{14}C counts were measured by liquid scintillation (Beckman Coulter, Fullerton, CA). Total uptake was measured in the presence of sodium. Non-transporter mediated histidine uptake, leucine uptake not mediated by system L, and unspecific binding was measured in the presence of 8.6 mM 2-amino-2-norbornanecarboxylic acid (BCH, an amino acid analogue exclusively transported by system L) and in absence of sodium. Non-transporter mediated uptake and unspecific binding were subtracted from total uptake as a measure of transporter mediated histidine uptake or system L activity. Transporter activities were expressed as pmol/(mg membrane protein x 300 seconds).

Na^+K^+-ATPase activity

Total ATPase/GTPase activity was measured in sarcolemma using a commercially available kit (ATPase/GTPase Activity Assay Kit, Sigma Aldrich) utilizing colorimetric assessment of free phosphate. Samples containing 0.5 μg of sarcolemmal protein were mixed with assay buffer and 10 μL of 4 mM ATP (Sigma Aldrich). Samples were incubated for 150 seconds. Color reagent was added, and samples were incubated for 30 minutes. Absorbance at 620 nm was measured using a spectrometer (Spectramax, Molecular Devices, San Jose, CA). Ouabain sensitive ATPase activity was measured similarly except samples containing 0.5 μg of sarcolemmal protein were incubated with 10 μL of 3 mM ouabain (Sigma Aldrich) for 30 minutes prior to incubation with ATP. Samples were run in triplicate and averaged. The

difference between total ATPase activity and ATPase activity in the presence of ouabain was taken as Na^+K^+-ATPase activity.

ATP content

ATP content was quantified in muscle biopsy samples from biceps femoris muscle. Fifty mg of muscle was combined with 0.25 mL of 70% methanol and 100 μL of the internal standard ATP-d4 (Cambridge Isotope Laboratories, Tewksbury, MA) (250ug/mL in 1:1 methanol to water). Samples were homogenized for 2 minutes and centrifuged at 17,000 g for 5 minutes at 4°C. The supernatant was collected and saved on ice. The pellet was combined with 0.25 mL of 100% methanol then homogenized for 2 minutes and centrifuged at 17,000 g for 5 minutes at 4°C. The supernatant was collected and combined with the previously collected supernatant; this was centrifuged at 17,000 g for 5 minutes at 4°C. LC/MS/MS quantitation of ATP was performed according to previous studies with modifications (Bustamante et al., 2017). Chromatographic separation was performed on a 1200 series HPLC (Agilent, Santa Clara, CA) using a 100X2 mm 5 um Luna NH2 column (Phenomenex, Torrance, CA) operated in HILIC mode. Buffer A consisted of 100% acetonitrile, and buffer B consisted of 95:5 water with 20 mM ammonium acetate adjusted to pH 9.6 with 20 mM ammonium hydroxide. Two uL of the extracted sample was analyzed using the following gradient at a flow rate of 0.6 mL/min: linear gradient from 5–100% B over 6 minutes, hold at 100% B from 6–9.5 minutes, then 100–5% B from 9.5–10.5 minutes, followed by re-equilibration at 5% B from 10.5–14 minutes. The column temperature was held at 15°C for the entire gradient. Mass spectrometric analysis was performed on an Agilent 6410 triple quadrupole mass spectrometer in positive ionization mode. The drying gas was 300°C at a flow rate of 12 mL/min. The nebulizer pressure was 30 psi. The capillary voltage was 4000 V. Data for ATP was acquired in MRM mode using experimentally optimized collision energies obtained by flow injection analysis of authentic standards. Calibration standards were analyzed over a range of concentrations from 0.1–100 ng on column. Calibration curves for ATP were constructed using Agilent Masshunter Quantitative Analysis software. Results for muscle tissue were quantitated using the calibration curves to obtain the on column concentration, followed by normalization of the results using the sample weight.

Statistical analysis

Student's t-test was used to compare groups. A Mann-Whitney test was used in cases of non-normally distributed data. Data were analyzed using GraphPad Prism software (GraphPad, San Diego, CA). Values are reported as mean ± SD. A P value of ≤0.05 was considered statistically significant. Given that comparisons were ordered based on priority and planned *a priori* at the time of study design, we did not adjust for multiple comparisons.

RESULTS

Fetal and hindlimb weights, arterial blood gases, and hormone concentrations are shown in Table #3 and were previously reported elsewhere (Rozance et al., 2018; Wai et al., 2018) but are presented here for the purpose of describing the IUGR phenotype. Fetal weight was 43% lower in the IUGR group (P<0.0001), and the IUGR hindlimb weight was 46% lower than

CON (P<0.0001). External iliac arterial and femoral venous potassium concentrations were significantly higher in IUGR vs CON (P<0.05; Figure 3).

We measured mRNA expression of several key amino acid transporters from system A, N, and L families of amino acid transporters. mRNA expression levels of system A amino acid transporters *SLC38A2* and *SLC38A4* were 35% and 44% lower, respectively, in IUGR muscle compared to CON (P<0.05). mRNA expression levels of system N transporters *SLC38A3, SLC38A5*, and *SLC38A7* and system L transporters *SLC7A5* and *SLC7A8* and associated heavy chain, *SLC3A2*, were similar between groups (Figure 4).

Despite lower mRNA expression of *SLC38A2* and *SLC38A4* in IUGR muscle, transporter mediated histidine uptake and system L activity in sarcolemma were similar between CON and IUGR groups (Figure 5A&B). However, sarcolemmal Na^+K^+-ATPase activity was lower by 64% in IUGR compared to CON (P<0.05; Figure 5C). Na^+K^+-ATPase α1 and β1 subunit expression levels were similar between CON and IUGR samples (Figure 6). ATP content was lower by 25% in IUGR muscle tissue compared to CON (P<0.05; Figure 7).

Relative protein expression levels of total and phosphorylated AKT (Ser 473), 4E-BP1 (Thr 37/46 and Thr 70), eIF2α (Ser 51), AMPKα (Thr 172), p70 S6 kinase (Thr 421/Ser424) and rpS6 (Ser 235/236) were similar between CON and IUGR muscle homogenate (Figure 8).

DISCUSSION

The goal of this study was to determine a potential mechanism to explain our previously published findings that weight-specific net total amino acid uptake by the fetal sheep hindlimb *in vivo* is markedly lower in the IUGR fetus compared to normally-grown controls (Rozance et al., 2018). To accomplish this, we first measured the *ex vivo* activity of amino acid transporters in sarcolemma isolated from hindlimb muscle. Despite lower mRNA expression of *SLC38A2* and *SLC38A4* in IUGR muscle, the transporter mediated histidine uptake was similar in control versus IUGR muscle sarcolemma. We also found that system L transporter mRNA expression and activity were similar in control versus IUGR sarcolemma. However, ouabain-inhibitable sarcolemmal ATPase activity, a readout of Na^+K^+-ATPase activity, was significantly lower in IUGR versus control, a finding indirectly supported by higher arterial and venous potassium concentrations in IUGR fetal sheep compared to control. Our current results suggest that reduced sarcolemmal Na^+K^+-ATPase activity in skeletal muscle of IUGR fetuses decreases the driving force for sodium dependent amino acid transporters such as system A and N, thereby lowering their activity *in vivo.* This, in turn, would indirectly lower *in vivo* system L activity by reducing cytosolic concentrations of non-essential neutral amino acids (Figure 1). We also found reduced ATP content in IUGR skeletal muscle, which could further reduce *in vivo* Na^+K^+-ATPase activity and subsequent amino acid transporter activity.

Previously, we measured substrates transported across the hindlimb circulation *in vivo* and found a selective reduction in amino acid uptake rates in IUGR. Using leucine as a stable isotope tracer *in vivo*, we showed that leucine transport inward and outward across the IUGR hindlimb muscle was reduced, as was net amino acid uptake (Rozance et al., 2018).

One possible explanation for these previous findings is that IUGR is associated with reduced activity of amino acid transporters in the muscle sarcolemma. To test this hypothesis, we developed novel methods to isolate fetal sheep sarcolemma from muscle biopsy samples and measured uptake of amino acid tracers in this sarcolemma. We elected to focus on the transporter mediated uptake of histidine (representing the activity of several transporter systems including system A and N) and system L activity, because these systems are believed to constitute the main transporters mediating amino acid uptake in muscle cells (Barker & Ellory, 1990; Dickinson & Rasmussen, 2013). Histidine is an essential amino acid that is taken up into cells by many of the 11 members of the *SLC38* family of sodium–amino acid co-transporters, including the system A amino acid transporter isoform SNAT2 and the system N transporter isoform SNAT3 (Broer, 2014) as well as by system L (Meier et al., 2002). Thus, transporter mediated histidine uptake represents a functional readout of several key amino acid uptake transporters. In addition, we measured BCH-inhibitable leucine uptake, which is a specific assay for system L transporter activity. IUGR has been reported to be associated with lower protein expression and activity of system A and L amino acid transporter isoforms in human (Jansson & Powell, 2006) and baboon (Pantham et al., 2015) trophoblast microvillous plasma membranes *in vitro*, and lower placental capacity to transport essential amino acids in animal experiments *in vivo* (Ross et al., 1996; Anderson et al., 1997; de Vrijer et al., 2004; Pantham et al., 2015). Contrary to our hypothesis, optimal transporter mediated uptake of histidine and system L activity *ex vivo* did not differ between control and IUGR sarcolemma, suggesting that the intrinsic transporter capacity, including system A, N, and L activity, is unaltered in IUGR skeletal muscle. The observed unchanged transporter mediated histidine uptake in the sarcolemma despite lower *SLC38A2* and *SLC38A4* mRNA expression in muscle biopsies may be explained by reports that modulation of transporter trafficking to the plasma membrane, rather than changes in gene transcription, constitute the predominant mechanism regulating system A transporter activity (Rosario et al., 2013; Chen et al., 2015; Rosario et al., 2016).

Members of the *SLC38* family co-transport sodium and amino acids into the cell utilizing the energy stored by the inwardly directed sodium gradient across the sarcolemma. Na^+K^+-ATPase is ubiquitously expressed and responsible for maintaining this sodium gradient (Clausen, 2003). In this study, we found that sarcolemmal Na^+K^+-ATPase activity *ex vivo* was significantly lower in IUGR as compared to control muscle, which could have contributed to the reduced *in vivo* muscle amino acid uptake that we previously reported (Rozance et al., 2018). Indeed, inhibition of Na^+K^+-ATPase by ouabain markedly decreases basal system A activity in rat extensor digitorum longus (EDL) muscle (Guma et al., 1988), the isolated perfused rat hindquarter (Zorzano et al., 1986), cultured human umbilical endothelial cells (Lau et al., 1994), the exocrine pancreas (Norman & Mann, 1987), and human placental fragments (Shibata et al., 2006). In addition, *in vitro* Na^+K^+-ATPase activity has been reported to be lower in trophoblast plasma membranes of the human IUGR placenta (Johansson et al., 2003). Therefore, we speculate that reduced sarcolemmal Na^+K^+-ATPase activity in the muscle of IUGR fetuses contributes to reduced *in vivo* amino acid uptake rates by decreasing the driving force for sodium dependent amino acid transporters such as system A. Additionally, lower system A activity indirectly lowers *in vivo* system L activity by reducing cytosolic concentrations of non-essential neutral amino acids (Figure 1).

We observed higher external iliac arterial and femoral venous potassium concentrations in IUGR fetal blood compared to controls, which is consistent with reduced Na^+K^+-ATPase activity. Blood pH was slightly lower in IUGR, which also could contribute to increased potassium concentrations. However, based on expected differences in circulating potassium caused by changes in pH, this is unlikely (Burnell et al., 1956). System A activity is highly sensitive to changes in pH within the physiological range with inhibition of transporter activity at lower pH (Broer, 2014). Thus, it is possible that lower extracellular pH in IUGR muscle, as indicated by the lower blood pH, also may contribute to inhibition of system A activity *in vivo*. Whether other organ systems in the IUGR fetus might also be affected by lower Na^+K^+-ATPase activity requires further investigation.

Several key activators of Na^+K^+-ATPase, such as growth factors and oxygen concentrations (Clausen & Hansen, 1977; Dorup & Clausen, 1995; Green et al., 2000) are known to be lower in the IUGR fetus compared to normally growing control fetuses (Rozance et al., 2018). For example, insulin and insulin-like growth factor 1 (IGF-1) stimulate activity of Na^+K^+-ATPase in muscle (Clausen & Hansen, 1977; Dorup & Clausen, 1995; Clausen, 2003). Insulin has two mechanisms to increase the activity of Na^+K^+-ATPase. First, insulin activates protein kinase C (PKC), which then phosphorylates and inactivates phospholemman, an inhibitor of Na^+K^+-ATPase (Walaas et al., 1994; Bibert et al., 2008; Pirkmajer & Chibalin, 2016). Second, insulin stimulates the translocation of Na^+K^+-ATPase to the plasma membrane (Hundal et al., 1992; Chibalin et al., 2001; Al-Khalili et al., 2004; Pirkmajer & Chibalin, 2016). We did not observe differences in the protein expression of $\alpha 1$ and $\beta 1$ subunits of Na^+K^+-ATPase in the sarcolemma, favoring covalent or post-translational modifications of the transporter rather than changes in localization of the protein. Hypoxia is also known to lower Na^+K^+-ATPase concentrations in the skeletal muscle of humans exposed to high altitude (Green et al., 2000). Future studies are needed to further define the regulatory mechanisms responsible for reduced *ex vivo* Na^+K^+-ATPase activity in hindlimb muscle sarcolemma in the IUGR fetus.

We further investigated whether limitations in intracellular ATP concentrations in IUGR muscle could be contributing to lower Na^+K^+-ATPase activity *in vivo*. Using highly specific mass spectrometry based methods for measuring ATP, we found a reduction in ATP content in IUGR skeletal muscle compared to control. ATP production largely occurs in the mitochondrial membrane via ATP synthase, and there is evidence that adult rats with a history of IUGR demonstrate lower mitochondrial respiration and ATP production in skeletal muscle, in conjunction with a phenotype of insulin resistance (Selak et al., 2003). Reduced mitochondrial respiration also could account for lower weight-specific oxygen consumption rates that we have previously found in the IUGR fetal hindlimb (Rozance et al., 2018), but future studies are needed to evaluate mitochondrial function in fetal IUGR skeletal muscle. This reduction in ATP content in skeletal muscle could contribute to reduced Na^+K^+-ATPase activity and subsequently lower hindlimb amino acid uptake *in vivo*. However, decreased ATP content does not exclusively account for the reduction we found in *ex vivo* Na^+K^+-ATPase activity, as ample ATP was supplied during the experimental procedure. We propose that both reduced muscle ATP content and post-translational modifications of Na^+K^+-ATPase contribute to lower activity *in vivo*, though further studies

are required to determine the relative contribution of these factors to Na^+K^+-ATPase activity in IUGR muscle.

Amino acid availability is an important regulator of pathways that are involved in protein synthesis and cellular growth, such as mechanistic target of rapamycin (mTOR) and general control nonrepressed (GCN) pathways. Amino acid transporters are now implicated in amino acid sensing and subsequent activation of cellular regulatory pathways (Hundal & Taylor, 2009). Within the cell, activation of mTORC1 leads to phosphorylation of 4E-BP1, which activates mRNA translation, and p70 S6 kinase, which in turn phosphorylates ribosomal protein S6, part of the 40S ribosomal subunit (Wang & Proud, 2006; Bahrami et al., 2014). Insulin stimulation also leads to activation of AKT and down-stream activation of mTORC1. AMPK inhibits mTORC1 during periods of lower energy availability and is known to regulate muscle protein synthesis (Goodman et al., 2011). Amino acid deprivation activates the GCN2 pathway, leading to phosphorylation of eIF2α and lower mRNA translation (Hundal & Taylor, 2009). We demonstrate similar protein expression of both total and phosphorylated AKT, 4E-BP1, eIF2α, AMPKα, p70 S6 kinase, and rpS6 in control and IUGR skeletal muscle, indicating that despite reduced amino acid uptake and muscle protein synthesis rates in the IUGR fetal hindlimb, the activity of key pathways involved in the regulation of protein synthesis were unaltered in late gestation. However, the initial step in mRNA translation involves the ATP-dependent activation of amino acids by aminoacyl-tRNA synthetases (Francklyn et al., 2008). In addition, protein synthesis is dependent on the availability of amino acids. Thus, we speculate that lower availability of ATP and lower amino acid uptake rates in IUGR skeletal muscle reduce protein synthesis in the IUGR muscle.

One of the limitations of the study was that we were unable to measure protein expression of sarcolemmal amino acid transporter isoforms such as SNAT2, LAT1, and LAT2 using western blot analysis due to lack of cross-reactivity to sheep of available antibodies. However, given the unchanged amino acid transporter activity, we believe that this limitation is minor. We were also unable to measure activity of individual amino acid transporter systems separately due to the small amount of sarcolemma available. Finally, due to limitations in the amount of muscle available, we used two different muscles – biceps femoris and gastrocnemius – for these studies. Both of these muscles are mixed fiber type muscles; however, we cannot exclude the possibility that individual muscles respond differently to the IUGR phenotype.

In conclusion, we demonstrated that *ex vivo* transporter mediated histidine uptake capacity and activity of system L amino acid transporters in sarcolemma from IUGR skeletal muscle is similar to control. However, reduced activity of Na^+K^+-ATPase in skeletal muscle sarcolemma and lower skeletal muscle ATP content could contribute to reduced *in vivo* uptake of amino acids by the IUGR hindlimb that we have previously demonstrated (Rozance et al., 2018). Lower ATP content may also indicate mitochondrial dysfunction in IUGR skeletal muscle; further investigation will be required to comprehensively measure mitochondrial function in fetal IUGR skeletal muscle. Understanding the underlying mechanisms that lead to reduced amino acid utilization in IUGR skeletal muscle, and

ultimately, poor skeletal muscle growth in the IUGR fetus, is essential to develop treatments to improve muscle mass and lifelong health.

Acknowledgements:

The authors wish to thank the University of Colorado School of Pharmacy, Mass Spectrometry Facility for analyzing samples.

Funding: NIH R01-HD079404 (LDB), R01-DK088139 (PJR), R01-HD093701 (PJR), and T32HD007186 (JS trainee, PJR PD)

Author Profile:

Jane Stremming received her MD at Ohio State University and subsequently completed a residency in Pediatrics at Emory University. She recently completed a fellowship in Neonatology at the University of Colorado. Her research and clinical interests are in fetal and neonatal nutrition and growth, and she is currently studying amino acid transport in skeletal muscle using a sheep model of intrauterine growth restriction.

References

Ahmed A, Taylor PM & Rennie MJ. (1990). Characteristics of glutamine transport in sarcolemmal vesicles from rat skeletal muscle. The American journal of physiology 259, E284–291. [PubMed: 2116727]

Al-Khalili L, Kotova O, Tsuchida H, Ehren I, Feraille E, Krook A & Chibalin AV. (2004). ERK1/2 mediates insulin stimulation of Na(+),K(+)-ATPase by phosphorylation of the alpha-subunit in human skeletal muscle cells. The Journal of biological chemistry 279, 25211–25218. [PubMed: 15069082]

Anderson AH, Fennessey PV, Meschia G, Wilkening RB & Battaglia FC. (1997). Placental transport of threonine and its utilization in the normal and growth-restricted fetus. The American journal of physiology 272, E892–900. [PubMed: 9176191]

Bahrami BF, Ataie-Kachoie P, Pourgholami MH & Morris DL. (2014). p70 Ribosomal protein S6 kinase (Rps6kb1): an update. Journal of clinical pathology 67, 1019–1025. [PubMed: 25100792]

Barker GA & Ellory JC. (1990). The identification of neutral amino acid transport systems. Experimental physiology 75, 3–26. [PubMed: 2178639]

Bell AW, Wilkening RB & Meschia G. (1987). Some Aspects of Placental Function in Chronically Heat-Stressed Ewes. J Dev Physiol 9, 17–29. [PubMed: 3559063]

Bibert S, Roy S, Schaer D, Horisberger JD & Geering K. (2008). Phosphorylation of phospholemman (FXYD1) by protein kinases A and C modulates distinct Na,K-ATPase isozymes. The Journal of biological chemistry 283, 476–486. [PubMed: 17991751]

Broer S (2014). The SLC38 family of sodium-amino acid co-transporters. Pflugers Archiv : European journal of physiology 466, 155–172. [PubMed: 24193407]

Brown LD & Hay WW Jr., (2016). Impact of placental insufficiency on fetal skeletal muscle growth. Molecular and cellular endocrinology 435, 69–77. [PubMed: 26994511]

Brown LD, Rozance PJ, Thorn SR, Friedman JE & Hay WW, Jr. (2012). Acute supplementation of amino acids increases net protein accretion in IUGR fetal sheep. American journal of physiology Endocrinology and metabolism 303, E352–364. [PubMed: 22649066]

Burnell JM, Scribner BH, Uyeno BT & Villamil MF. (1956). The effect in humans of extracellular pH change on the relationship between serum potassium concentration and intracellular potassium. The Journal of clinical investigation 35, 935–939. [PubMed: 13367188]

Bustamante S, Jayasena T, Richani D, Gilchrist RB, Wu LE, Sinclair DA, Sachdev PS & Braidy N. (2017). Quantifying the cellular NAD+ metabolome using a tandem liquid chromatography mass spectrometry approach. Metabolomics 14, 15. [PubMed: 30830318]

Bustin SA, Benes V, Garson JA, Hellemans J, Huggett J, Kubista M, Mueller R, Nolan T, Pfaffl MW, Shipley GL, Vandesompele J & Wittwer CT. (2009). The MIQE guidelines: minimum information for publication of quantitative real-time PCR experiments. Clin Chem 55, 611–622. [PubMed: 19246619]

Chen YY, Rosario FJ, Shehab MA, Powell TL, Gupta MB & Jansson T. (2015). Increased ubiquitination and reduced plasma membrane trafficking of placental amino acid transporter SNAT-2 in human IUGR. Clinical science (London, England : 1979) 129, 1131–1141.

Chibalin AV, Kovalenko MV, Ryder JW, Feraille E, Wallberg-Henriksson H & Zierath JR. (2001). Insulin- and glucose-induced phosphorylation of the Na(+),K(+)-adenosine triphosphatase alpha-subunits in rat skeletal muscle. Endocrinology 142, 3474–3482. [PubMed: 11459793]

Clausen T (2003). Na+-K+ pump regulation and skeletal muscle contractility. Physiological reviews 83, 1269–1324. [PubMed: 14506306]

Clausen T & Hansen O. (1977). Active Na-K transport and the rate of ouabain binding. The effect of insulin and other stimuli on skeletal muscle and adipocytes. The Journal of physiology 270, 415–430. [PubMed: 903900]

de Vrijer B, Regnault TR, Wilkening RB, Meschia G & Battaglia FC. (2004). Placental uptake and transport of ACP, a neutral nonmetabolizable amino acid, in an ovine model of fetal growth restriction. Am J Physiol 287, E1114-E1124.

Dickinson JM & Rasmussen BB. (2013). Amino acid transporters in the regulation of human skeletal muscle protein metabolism. Current opinion in clinical nutrition and metabolic care 16, 638–644. [PubMed: 24100668]

Dorup I & Clausen T. (1995). Insulin-like growth factor I stimulates active Na(+)-K+ transport in rat soleus muscle. The American journal of physiology 268, E849–857. [PubMed: 7762637]

Francklyn CS, First EA, Perona JJ & Hou YM. (2008). Methods for kinetic and thermodynamic analysis of aminoacyl-tRNA synthetases. Methods 44, 100–118. [PubMed: 18241792]

Gale CR, Martyn CN, Kellingray S, Eastell R & Cooper C. (2001). Intrauterine programming of adult body composition. The Journal of clinical endocrinology and metabolism 86, 267–272. [PubMed: 11232011]

Goodman CA, Mayhew DL & Hornberger TA. (2011). Recent progress toward understanding the molecular mechanisms that regulate skeletal muscle mass. Cellular signalling 23, 1896–1906. [PubMed: 21821120]

Green H, Roy B, Grant S, Burnett M, Tupling R, Otto C, Pipe A & McKenzie D. (2000). Downregulation in muscle Na(+)-K(+)-ATPase following a 21-day expedition to 6,194 m. Journal of applied physiology (Bethesda, Md : 1985) 88, 634–640.

Grundy D (2015). Principles and standards for reporting animal experiments in The Journal of Physiology and Experimental Physiology. The Journal of physiology 593, 2547–2549. [PubMed: 26095019]

Guma A, Testar X, Palacin M & Zorzano A. (1988). Insulin-stimulated alpha-(methyl)aminoisobutyric acid uptake in skeletal muscle. Evidence for a short-term activation of uptake independent of Na+ electrochemical gradient and protein synthesis. The Biochemical journal 253, 625–629. [PubMed: 2460082]

Hundal HS, Marette A, Mitsumoto Y, Ramlal T, Blostein R & Klip A. (1992). Insulin induces translocation of the alpha 2 and beta 1 subunits of the Na+/K(+)-ATPase from intracellular compartments to the plasma membrane in mammalian skeletal muscle. The Journal of biological chemistry 267, 5040–5043. [PubMed: 1312081]

Hundal HS, Rennie MJ & Watt PW. (1987). Characteristics of L-glutamine transport in perfused rat skeletal muscle. The Journal of physiology 393, 283–305. [PubMed: 3328779]

Hundal HS & Taylor PM. (2009). Amino acid transceptors: gate keepers of nutrient exchange and regulators of nutrient signaling. American journal of physiology Endocrinology and metabolism 296, E603–613. [PubMed: 19158318]

Jansson T, Ekstrand Y, Bjorn C, Wennergren M & Powell TL. (2002). Alterations in the activity of placental amino acid transporters in pregnancies complicated by diabetes. Diabetes 51, 2214–2219. [PubMed: 12086952]

Jansson T & Powell TL. (2006). IFPA 2005 Award in Placentology Lecture. Human placental transport in altered fetal growth: does the placenta function as a nutrient sensor? -- a review. Placenta 27 Suppl A, S91–97. [PubMed: 16442615]

Johansson M, Karlsson L, Wennergren M, Jansson T & Powell TL. (2003). Activity and protein expression of Na+/K+ ATPase are reduced in microvillous syncytiotrophoblast plasma membranes isolated from pregnancies complicated by intrauterine growth restriction. The Journal of clinical endocrinology and metabolism 88, 2831–2837. [PubMed: 12788896]

Kavitha JV, Rosario FJ, Nijland MJ, McDonald TJ, Wu G, Kanai Y, Powell TL, Nathanielsz PW & Jansson T. (2014). Down-regulation of placental mTOR, insulin/IGF-I signaling, and nutrient transporters in response to maternal nutrient restriction in the baboon. FASEB journal : official publication of the Federation of American Societies for Experimental Biology 28, 1294–1305. [PubMed: 24334703]

Kensara OA, Wootton SA, Phillips DI, Patel M, Jackson AA & Elia M. (2005). Fetal programming of body composition: relation between birth weight and body composition measured with dual-energy X-ray absorptiometry and anthropometric methods in older Englishmen. The American journal of clinical nutrition 82, 980–987. [PubMed: 16280428]

Klip A, Ramlal T, Young DA & Holloszy JO. (1987). Insulin-induced translocation of glucose transporters in rat hindlimb muscles. FEBS letters 224, 224–230. [PubMed: 2960560]

Lau YT, Chen JK, Chen BS & Hsieh CC. (1994). Transport of 2-aminoisobutyric acid in cultured endothelial cells. Biochimica et biophysica acta 1194, 118–122. [PubMed: 8075124]

Mackenzie B & Erickson JD. (2004). Sodium-coupled neutral amino acid (System N/A) transporters of the SLC38 gene family. Pflugers Archiv : European journal of physiology 447, 784–795. [PubMed: 12845534]

Meier C, Ristic Z, Klauser S & Verrey F. (2002). Activation of system L heterodimeric amino acid exchangers by intracellular substrates. The EMBO journal 21, 580–589. [PubMed: 11847106]

Norman PS & Mann GE. (1987). Ionic dependence of amino-acid transport in the exocrine pancreatic epithelium: calcium dependence of insulin action. The Journal of membrane biology 96, 153–163. [PubMed: 3110421]

Pantham P, Rosario FJ, Nijland M, Cheung A, Nathanielsz PW, Powell TL, Galan HL, Li C & Jansson T. (2015). Reduced placental amino acid transport in response to maternal nutrient restriction in the baboon. American journal of physiology Regulatory, integrative and comparative physiology 309, R740–746.

Pirkmajer S & Chibalin AV. (2016). Na,K-ATPase regulation in skeletal muscle. American journal of physiology Endocrinology and metabolism 311, E1–e31. [PubMed: 27166285]

Regnault TR, de Vrijer B, Galan HL, Wilkening RB, Battaglia FC & Meschia G. (2013). Umbilical uptakes and transplacental concentration ratios of amino acids in severe fetal growth restriction. Pediatr Res 73, 602–611. [PubMed: 23407119]

Rosario FJ, Dimasuay KG, Kanai Y, Powell TL & Jansson T. (2016). Regulation of amino acid transporter trafficking by mTORC1 in primary human trophoblast cells is mediated by the ubiquitin ligase Nedd4–2. Clinical science (London, England : 1979) 130, 499–512.

Rosario FJ, Kanai Y, Powell TL & Jansson T. (2013). Mammalian target of rapamycin signalling modulates amino acid uptake by regulating transporter cell surface abundance in primary human trophoblast cells. The Journal of physiology 591, 609–625. [PubMed: 23165769]

Ross JC, Fennessey PV, Wilkening RB, Battaglia FC & Meschia G. (1996). Placental transport and fetal utilization of leucine in a model of fetal growth retardation. Am J Physiol 270, E491–E503. [PubMed: 8638698]

Rozance PJ, Zastoupil L, Wesolowski SR, Goldstrohm DA, Strahan B, Cree-Green M, Sheffield-Moore M, Meschia G, Hay WW Jr., Wilkening RB & Brown LD (2018). Skeletal muscle protein accretion rates and hindlimb growth are reduced in late gestation intrauterine growth-restricted fetal sheep. The Journal of physiology 596, 67–82. [PubMed: 28940557]

Selak MA, Storey BT, Peterside I & Simmons RA. (2003). Impaired oxidative phosphorylation in skeletal muscle of intrauterine growth-retarded rats. American journal of physiology Endocrinology and metabolism 285, E130–137. [PubMed: 12637257]

Sharma D, Shastri S & Sharma P. (2016). Intrauterine Growth Restriction: Antenatal and Postnatal Aspects. Clinical medicine insights Pediatrics 10, 67–83. [PubMed: 27441006]

Shibata E, Powers RW, Rajakumar A, von Versen-Hoynck F, Gallaher MJ, Lykins DL, Roberts JM & Hubel CA. (2006). Angiotensin II decreases system A amino acid transporter activity in human placental villous fragments through AT1 receptor activation. American journal of physiology Endocrinology and metabolism 291, E1009–1016.

Srikanthan P & Karlamangla A. (2011). Relative muscle mass is inversely associated with insulin resistance and prediabetes. Findings from the third National Health and Nutrition Examination Survey. J Clin Endocrinol Metab 96, 2898–2903. [PubMed: 21778224]

Thorn SR, Rozance PJ, Brown LD & Hay WW Jr., (2011). The intrauterine growth restriction phenotype: fetal adaptations and potential implications for later life insulin resistance and diabetes. Seminars in reproductive medicine 29, 225–236. [PubMed: 21710398]

Verrey F (2003). System L: heteromeric exchangers of large, neutral amino acids involved in directional transport. Pflugers Archiv : European journal of physiology 445, 529–533. [PubMed: 12634921]

Verrey F, Closs EI, Wagner CA, Palacin M, Endou H & Kanai Y. (2004). CATs and HATs: the SLC7 family of amino acid transporters. Pflugers Archiv : European journal of physiology 447, 532–542. [PubMed: 14770310]

Wai SG, Rozance PJ, Wesolowski SR, Hay WW Jr., & Brown LD (2018). Prolonged amino acid infusion into intrauterine growth restricted fetal sheep increases leucine oxidation rates. American journal of physiology Endocrinology and metabolism.

Walaas SI, Czernik AJ, Olstad OK, Sletten K & Walaas O. (1994). Protein kinase C and cyclic AMP-dependent protein kinase phosphorylate phospholemman, an insulin and adrenaline-regulated membrane phosphoprotein, at specific sites in the carboxy terminal domain. The Biochemical journal 304 (Pt 2), 635–640. [PubMed: 7999001]

Wang X & Proud CG. (2006). The mTOR pathway in the control of protein synthesis. Physiology (Bethesda, Md) 21, 362–369.

Whincup PH, Kaye SJ, Owen CG, Huxley R, Cook DG, Anazawa S, Barrett-Connor E, Bhargava SK, Birgisdottir BE, Carlsson S, de Rooij SR, Dyck RF, Eriksson JG, Falkner B, Fall C, Forsen T, Grill V, Gudnason V, Hulman S, Hypponen E, Jeffreys M, Lawlor DA, Leon DA, Minami J, Mishra G, Osmond C, Power C, Rich-Edwards JW, Roseboom TJ, Sachdev HS, Syddall H, Thorsdottir I, Vanhala M, Wadsworth M & Yarbrough DE. (2008). Birth weight and risk of type 2 diabetes: a systematic review. Jama 300, 2886–2897. [PubMed: 19109117]

Zorzano A, Balon TW, Goodman MN & Ruderman NB. (1986). Insulin and exercise stimulate muscle alpha-aminoisobutyric acid transport by a Na+-K+-ATPase independent pathway. Biochemical and biophysical research communications 134, 1342–1349. [PubMed: 2418838]

Key Points

- Fetuses with intrauterine growth restriction (IUGR) have reduced muscle mass that persists postnatally, which may contribute to their increased risk for adult onset metabolic diseases, such as diabetes and obesity.
- Amino acid transporter mediated histidine uptake and system L amino acid transporter activity were similar in sarcolemmal membranes isolated from control and IUGR hindlimb skeletal muscle.
- Activity of Na^+K^+-ATPase, which is responsible for establishing the sodium gradient necessary for system A and N amino acid transporter function, was significantly reduced in IUGR skeletal muscle sarcolemma compared to control.
- ATP content was lower in IUGR skeletal muscle.
- Expression and phosphorylation of proteins in the mTOR pathway were similar in control and IUGR skeletal muscle homogenate.
- Our data suggest that lower Na^+K^+-ATPase activity, which reduces the driving force for active amino acid transport, and lower ATP availability contribute to reduced amino acid uptake and protein synthesis in IUGR fetal skeletal muscle.

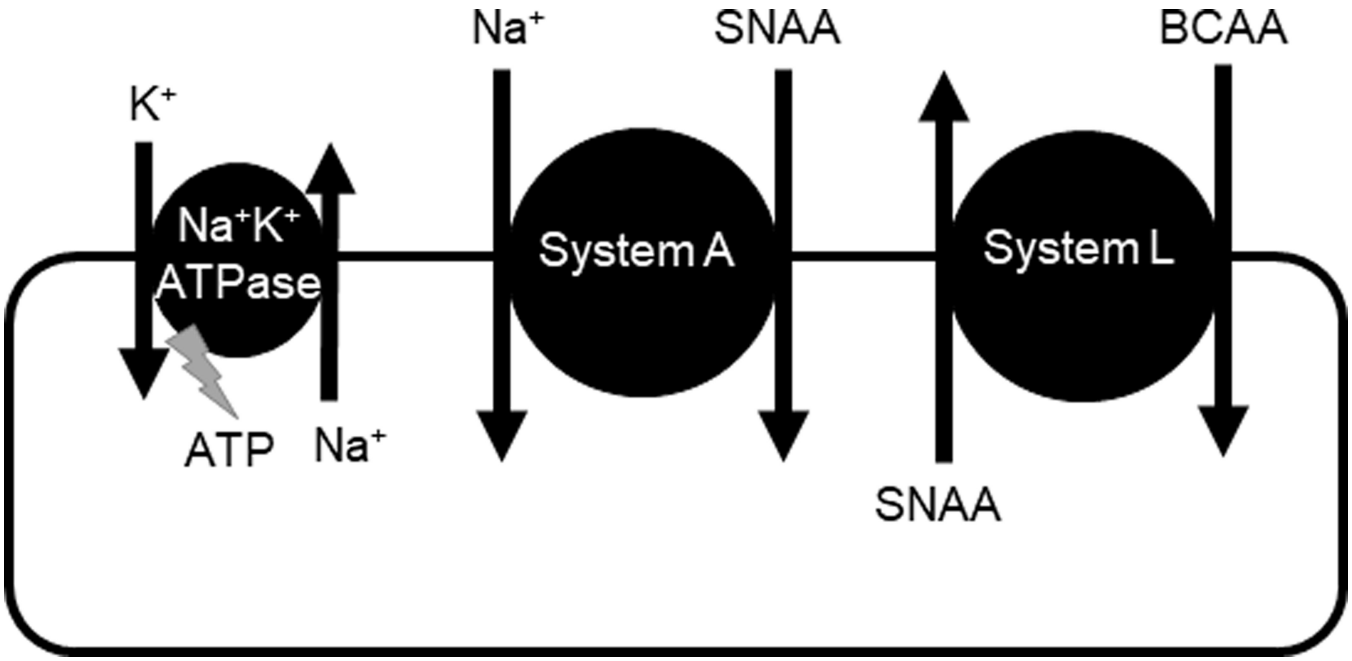

Figure 1. Relationship between Na^+K^+-ATPase and system A and L amino acid transporters

Na^+K^+-ATPase establishes a sodium gradient that is necessary for the function of system A transporters. System A transporters carry small neutral amino acids (SNAA) into the cell in cotransport with sodium. System L transporters exchange extracellular branched chain amino acids (BCAA) for intracellular SNAA.

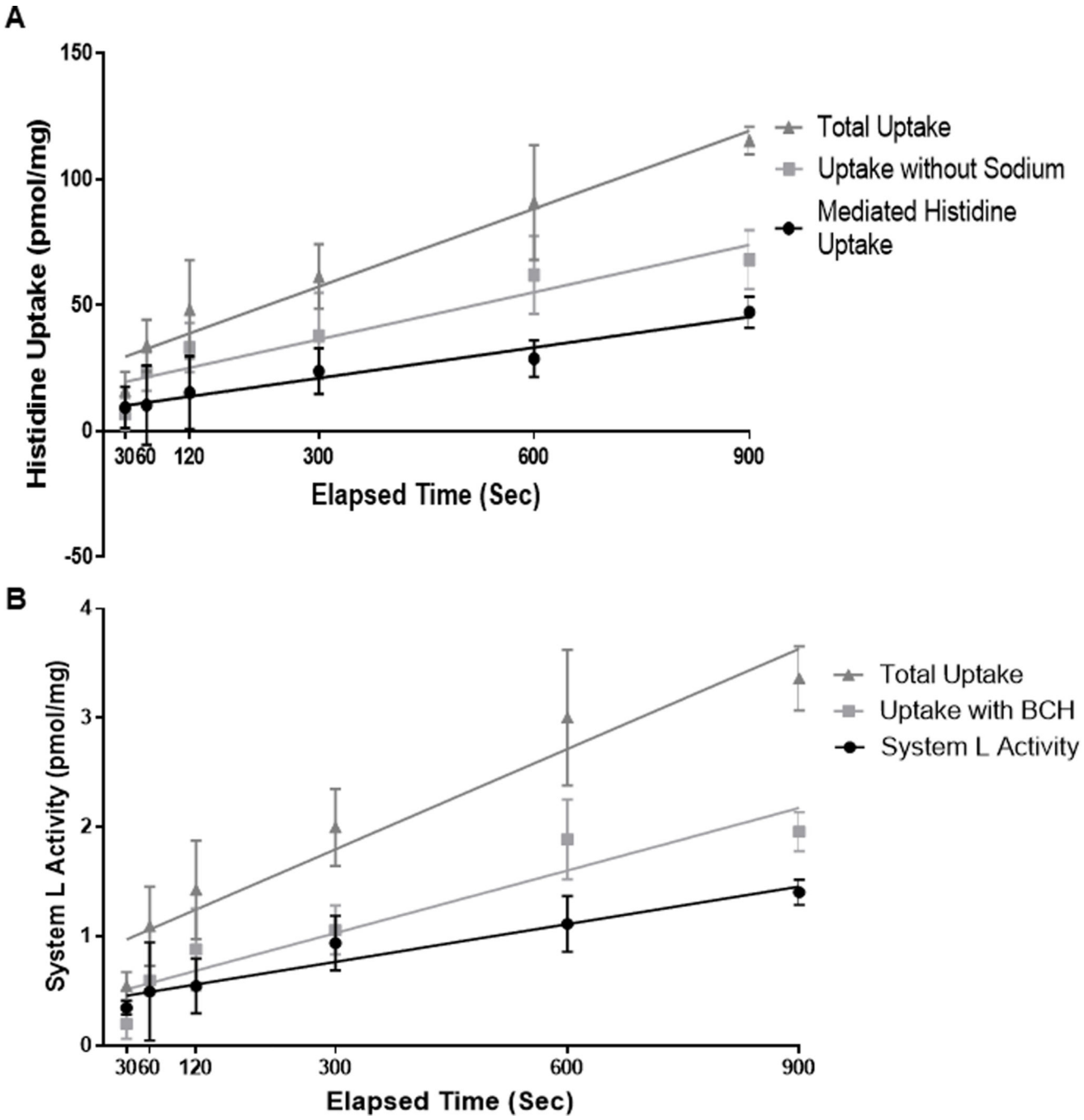

Figure 2. Time dependence of histidine uptake and system L activity (A)

(A) (▲) = Total histidine uptake; (■) = Sodium-independent histidine uptake plus unspecific binding; (•) = Mediated histidine uptake. (B) (▲) = Total leucine uptake; (■) = Uptake in the presence of BCH (2-amino-2-norbornanecarboxylic acid, an amino acid analogue exclusively transported by system L) representing leucine uptake not mediated by system L plus unspecific binding. (•) = BCH-inhibitable leucine uptake (system L activity). N=4 for 30,60,120, and 300 second time points or n=2 for 600 and 900 second time points. Histidine and leucine uptake were linear during the first 900 seconds.

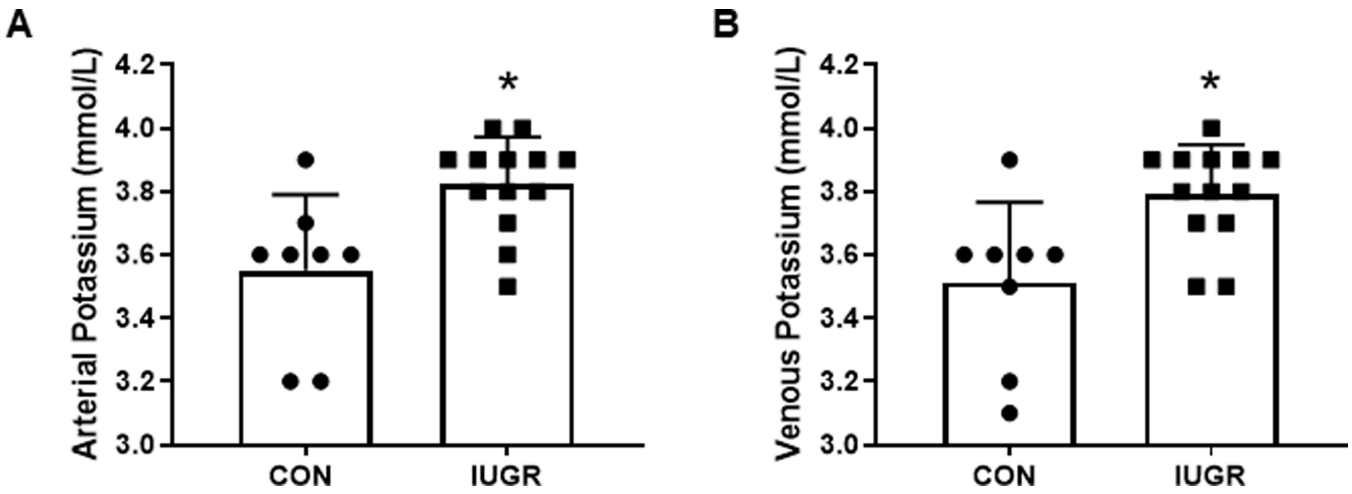

Figure 3. Arterial and venous potassium concentrations

Steady-state (A) external iliac arterial and (B) femoral venous blood concentrations of potassium in CON (•, n=8) and IUGR (■, n=13)fetal sheep at ~135dga. Individual animal data and mean ± SD are shown. **P*< 0.05 by Student's t-test.

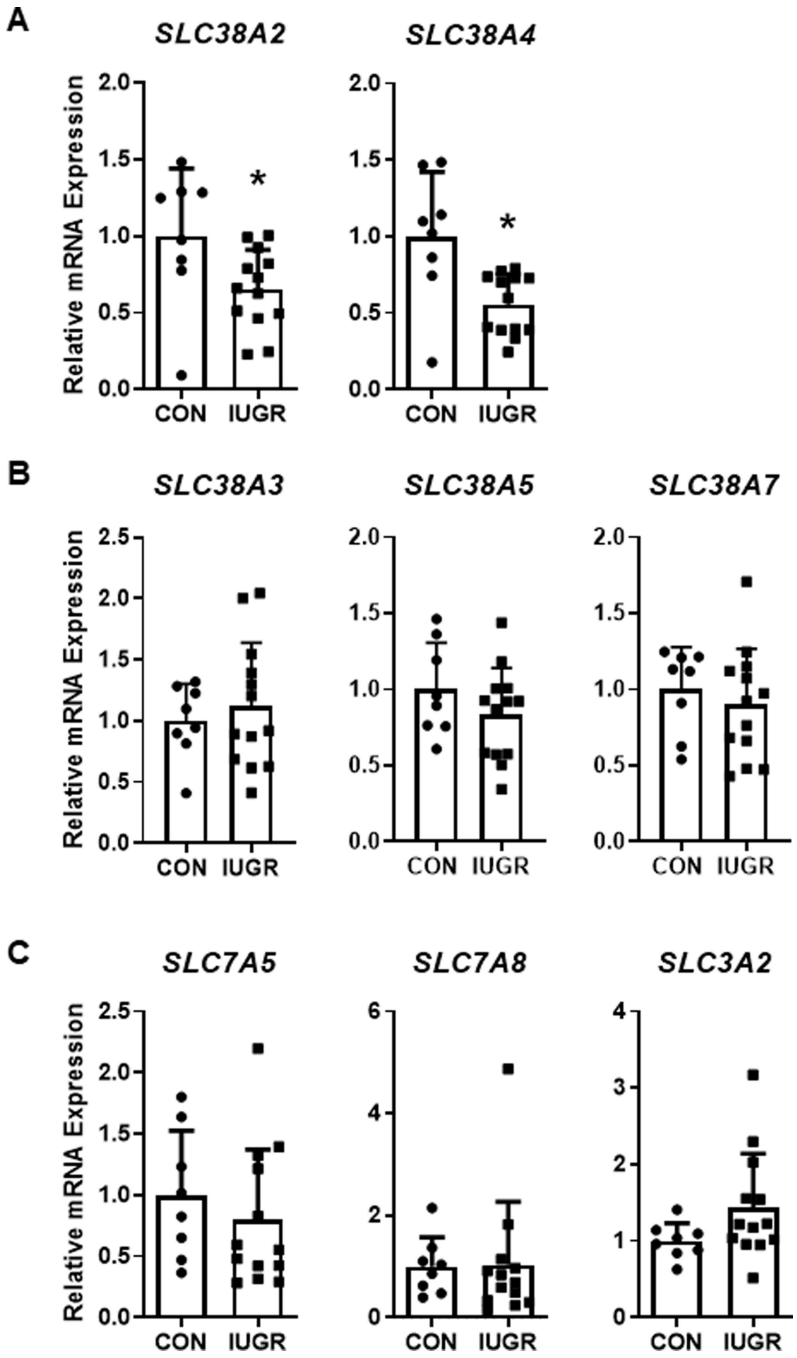

Figure 4. Expression of amino acid transporters in fetal skeletal muscle

mRNAexpression of (A) system A, (B) system N, and (C) system L transporters in CON (•, n=8) and IUGR (■, n=13) fetal bicepsfemoris muscle. Individual animal data and mean ± SD are shown. **P*<0.05 by Student's t-test or Mann Whitney test.

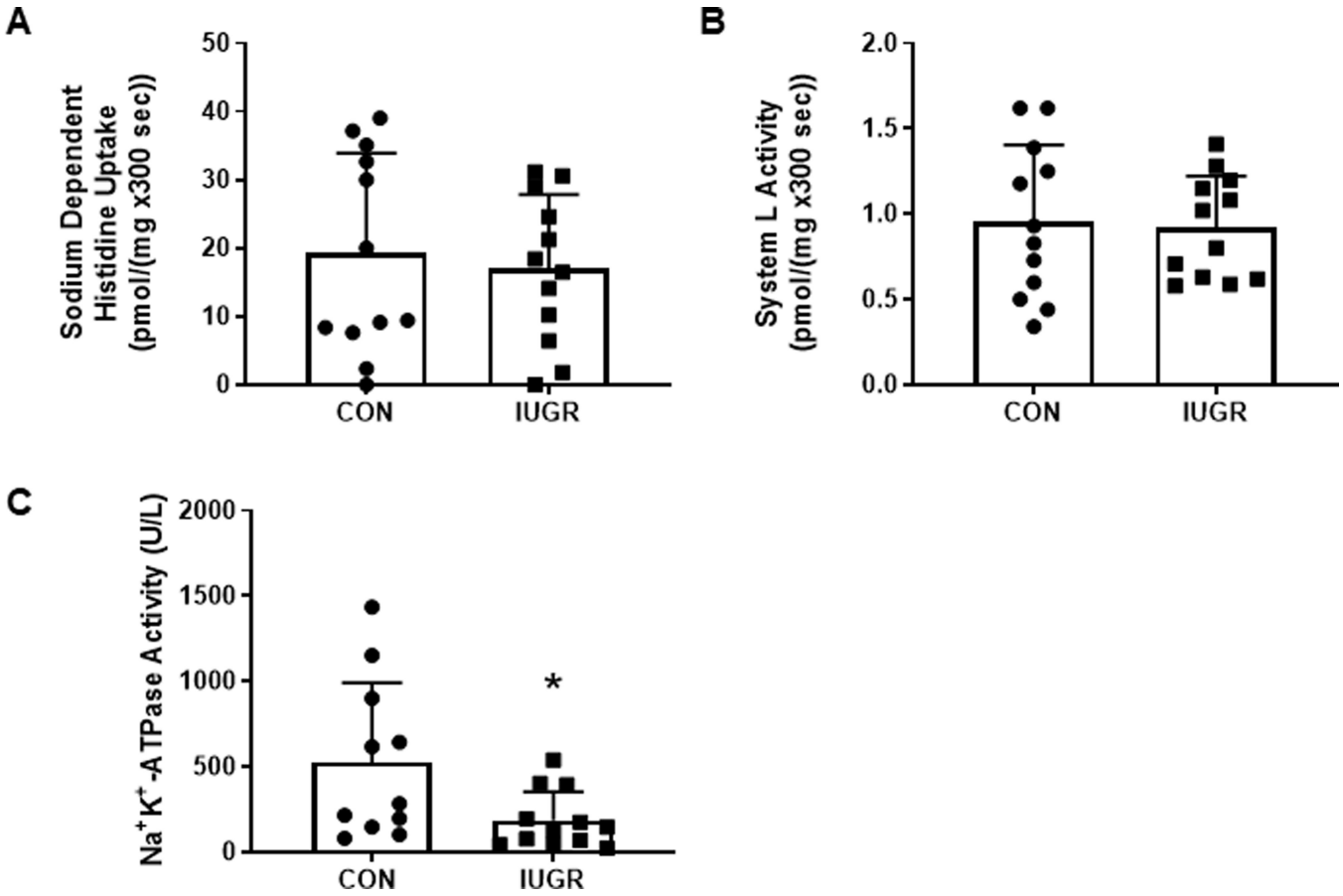

Figure 5. Sarcolemmal amino acid transporter and Na^+K^+-ATPase activity

(A) Sodium-dependent histidine uptake and (B) system L activity in CON (•, n=12) and IUGR (■, n=12) sarcolemmal vesicles, and (C) Na^+K^+-ATPase activity in CON (n=11) and IUGR (n=12) sarcolemmal vesicles isolated from gastrocnemius muscle. Individual animal data and mean ± SD are shown. *P< 0.05 by Mann Whitney test.

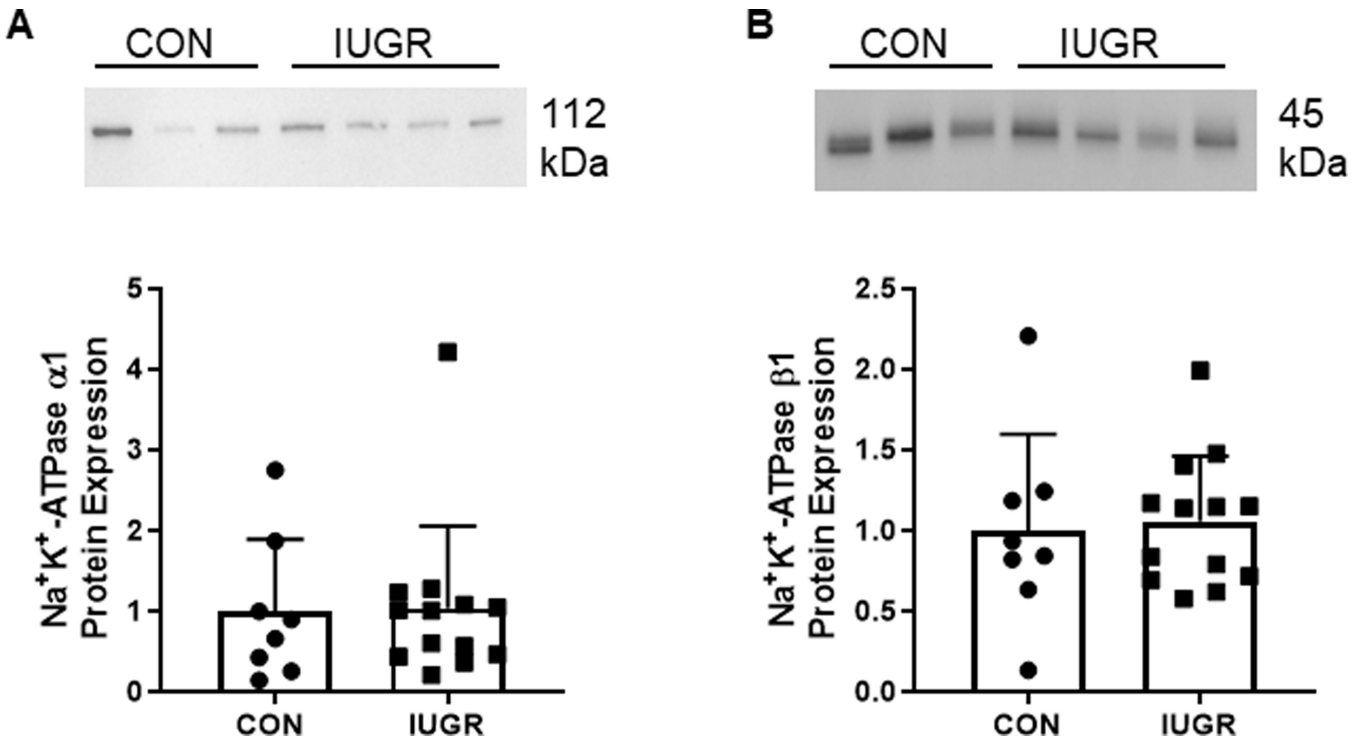

Figure 6. Expression of NaK-ATPase subunits in sarcolemma

Protein expression of (A) a1 and (B) (31 subunits of Na^+K^+-ATPase in CON (•, n=8) and IUGR (■, n=13) sarcolemma from gastrocnemius muscle. Representative blots are shown. Individual animal data and mean ± SD are shown.

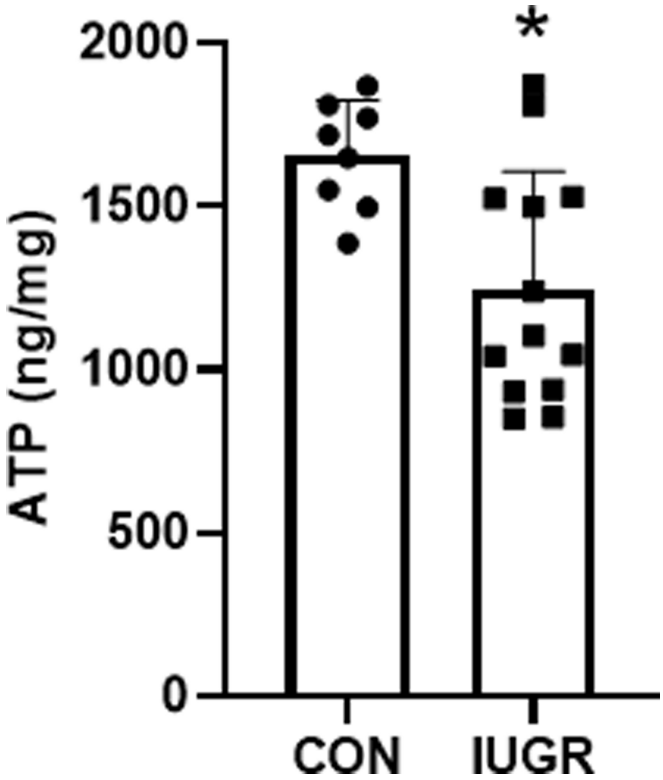

Figure 7. ATP content in fetal skeletal muscle

ATP content in CON (•, n=8) and IUGR (■, n=13) biceps femoris muscle. Individual animal data and mean ± SD are shown. *P< 0.05 by Student's t test.

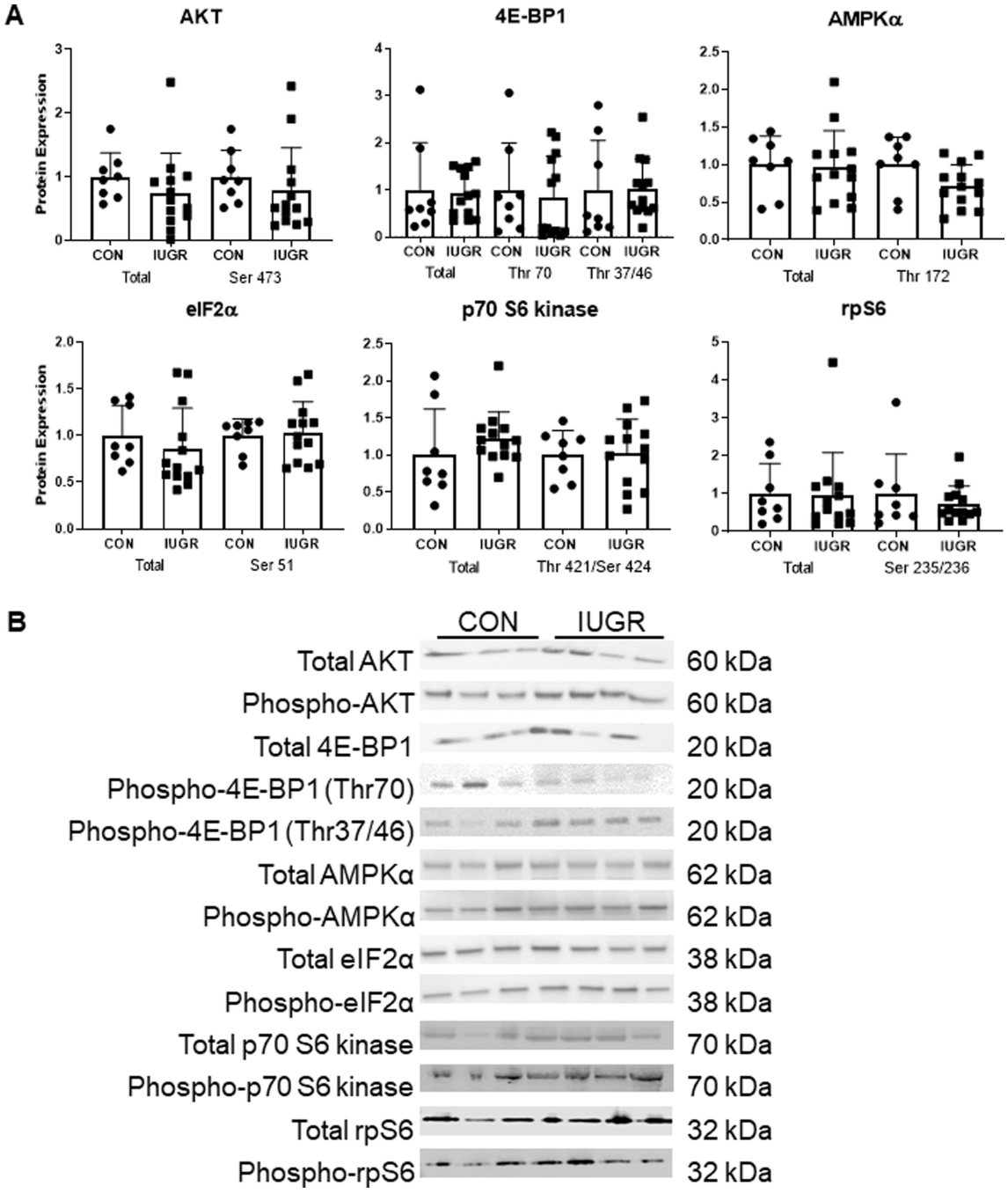

Figure 8. Expression of proteins regulating protein synthesis and cell growth

(A) Protein expression of AKT (Ser473), 4E-BP1 (Thr 70, Thr 37/46), AMPKa (Thr 172), eIF2a (Ser 51), p70 S6 kinase (Thr 421 /Ser424), and rpS6 (Ser 235/236) in CON (•, n=8) and IUGR (■, n=13) crude muscle homogenate. (B) Representative blots are shown. Individual animal data and mean ± SD are shown.

Table 1.

PCR Primer Forward (F') and Reverse (R') Sequences

Gene	F' Sequence	R' Sequence	Accession Number
SLC38A2	CTT GCC GCC CTC TTT GGA T	TAA CAC AGC CAG ACG GAC AA	NM_018976
SLC38A3	CTA CAC GGA GCT CAA GGA C	ACG GGT CCA CCT TGC TGT A	BT021187.1
SLC38A4	TTT GTA TGC CAC CCT GAG GTC CTT	AGA GGG CAG CAA GCA GAT ACA TGA	BC069819.1
SLC38A5	CTG TCT TCG TAC TCC ATC CA	CAG GAA AGT GGC GAT AAC CA	BC119859.1
SLC38A7	CCA GAA ATA TGC CAG CTT CC	GGT GGG CAT GGC ATT GAA C	NM_001100355.1
SLC7A5	GCT CGG CTT CAT CCA GAT C	AGG CAA AGA GGC CGC TGT A	NM_174613.2
SLC7A8	GGG CTT CAT CAA CTA CCT CTT C	GAA CAG CAG GCT GAC CTT AAT	NM_001192889
SLC3A2	TCC TGC ACT CTG CCA AGA AGA AGA	TGG ATT GAA ACC AAG GGT TCT GGC	BC003000.1

Table 2.

Antibody RRIDs

Na^+K^+-ATPase β1 Na^+K^+-ATPase α1 Total AKT Phospho-AKT Ser 473	US Biological Cat# A4000–72D, RRID:AB_2096644 US Biological Cat# A4000–52E, RRID:AB_2060978 Cell Signaling Technology Cat# 9272, RRID:AB_329827 Cell Signaling Technology Cat# 9271, RRID:AB_329825
Total 4E-BP1	Cell Signaling Technology Cat# 9452, RRID:AB_331692
Phospho-4E-BP1 Thr 37/46	Cell Signaling Technology Cat# 9459, RRID:AB_330985
Phospho-4E-BP1 Thr 70	Cell Signaling Technology Cat# 9455, RRID:AB_330949
Total eIF2α	Cell Signaling Technology Cat# 5324, RRID:AB_10692650
Phospho-eIF2α Ser 51	Cell Signaling Technology Cat# 9721, RRID:AB_330951
Total AMPKα Phospho-AMPKα Thr 172 Total p70 S6 kinase	Cell Signaling Technology Cat# 2532, RRID:AB_330331 Cell Signaling Technology Cat# 2535, RRID:AB_331250 Cell Signaling Technology Cat# 9202, RRID:AB_331676
Phospho-p70 S6 kinase Thr 421/Ser 424	Cell Signaling Technology Cat# 9204, RRID:AB_2265913
Total rpS6	Cell Signaling Technology Cat# 2217, RRID:AB_331355
Phospho-rpS6 Ser 235/236	Cell Signaling Technology Cat# 2211, RRID:AB_331679
HRP linked anti-mouse secondary	Cell Signaling Technology Cat# 7076, RRID:AB_330924
HRP linked anti-rabbit secondary	Cell Signaling Technology Cat# 7074, RRID:AB_2099233
IRDye 800CW anti-rabbit secondary	LI-COR Biosciences Cat# 926–32211, RRID:AB_621843

Table 3.

Fetal characteristics at time of study

	Control (n=12)	IUGR (n=13)	*P*-value
Fetal measurements			
Gestational age (d)	135 ± 1	134 ± 1	0.16
Fetal weight (g)	3423 ± 451	1961 ± 676	<0.0001
Hindlimb weight (g)	344 ± 47 †	185 ± 68	<0.0001
Hindlimb length (cm)	36.2 ± 2.2	29.0 ± 3.9	<0.0001
Gastrocnemius weight (g)	9.2 ± 1.1	5.0 ± 1.9	<0.0001
Biceps femoris weight (g)	18.9 ± 2.5 Δ	9.9 ± 3.4	<0.0001
Arterial pH	7.36 ± 0.01	7.34 ± 0.02	0.02
$PaCO_2$ (mmHg)	50.7 ± 1.7	51.5 ± 2.7	0.39
PaO_2 (mmHg)	20.1 ± 1.8	14.6 ± 3.1	<0.0001
SaO_2 (%)	47.2 ± 4.5	26.6 ± 11.6	<0.0001
Hematocrit (%)	34.0 ± 3.7	34.2 ± 5.0	0.92
Arterial blood O_2 content ($mmol \cdot L^{-1}$)	3.2 ± 0.5	1.9 ± 1.0	0.005
Plasma insulin ($ng \cdot ml^{-1}$)	0.34 ± 0.15	0.14 ± 0.07	0.0008
Plasma IGF-1 ($ng \cdot ml^{-1}$)	114.8 ± 38.5	43.6 ± 34.1	<0.0001

Values are means ± SD. *P*-values from Student's t-tests or Mann Whitney tests are shown.

† indicates n=8,

Δ indicates n=11